# An Enhanced Unified Space Vector Modulation Technique for Dual Converters with Isolated Voltage Supplies

*Zhen Huang[1], Tao Yang[1], Paolo Giangrande[1], Pat Wheeler[1], and Michael Galea[1,2]

[1]*Power Electronics, Machine and Control Group*
*University of Nottingham*
NG7 2RD, Nottingham
United Kingdom
*Zhen.Huang@nottingham.ac.uk

[2]*Key Laboratory of More Electric Aircraft Technology of Zhejiang Province*
*University of Nottingham Ningbo China*
315100, Ningbo
China

***Abstract*—This paper presents an enhanced modulation technique for dual converters with isolated supplies. This unified modulation technique is applicable for any positive voltage ratio between the isolated supplies. The modulation technique enhances the quality of converter output voltage. The effectiveness of the proposed technique is validated and results are presented for an open-end winding induction motor to demonstrate the advantages.**

***Index Terms*—Dual converter, multilevel converters, space vector modulation**

## I. Introduction

In the past two decades, dual converter topologies have been received increasing attention for motor drive applications [1]. This mainly results from its redundancy [2], fault-tolerance ability [3] and the possibility of generating more voltage levels for a given number of switches [4]. The dual converter employs two standard two-level or multilevel converters connecting to an open-end winding machine, as described in Fig.1.

According to their power supply arrangement, the dual converters generally feature three different configurations, which are dual converters with 1) isolated supplies, 2) one common source and 3) a floating bridge [1], [5]. The dual converter using a common voltage source requires to eliminate the zero-sequence current, while the dual converter with a floating bridge demands to regulate the capacitor voltage at the desired value. Consequently, both these two topologies result in relatively complex modulation schemes [1]. However, for the dual converter with two isolated supplies, the modulation method seems to be easier, due to the inherent nature of the power supplies arrangement (i.e. they are isolated). More importantly, this topology is able to provide a higher voltage for motor drives, that is critical especially for electric vehicle applications [6], grid-connected photovoltaic systems [7], etc.

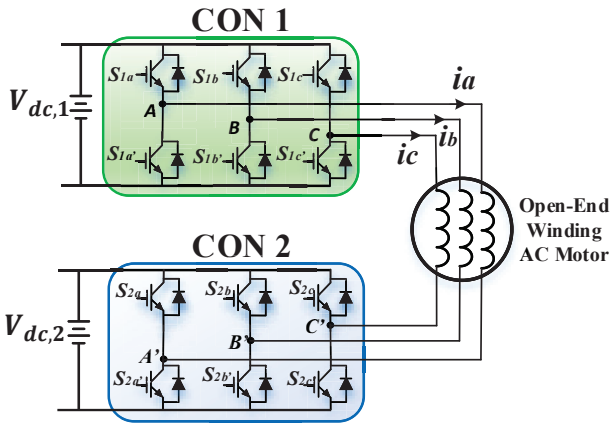


Fig. 1. Dual converter topology with isolated DC supplies.

Despite the rich redundant states available in dual converters, the modulation strategy to select appropriate states can be relatively complicated on the other side. In [8], a coordinated modulation technique is addressed for dual converters. It eliminates the need for trigonometric function calculations or sector identifications such that the computational burden is considerately relieved. However, this method is only applicable to symmetric voltage supplies, hence the voltages of CON1 and CON2 in Fig.1 are balanced. Actually, for drive applications such as electric vehicles [6], the voltage ratio is usually not constant, since the state of charge (SoC) of battery

This work was supported by the Natural Science Foundation of China under the grant with project code 51850410515.

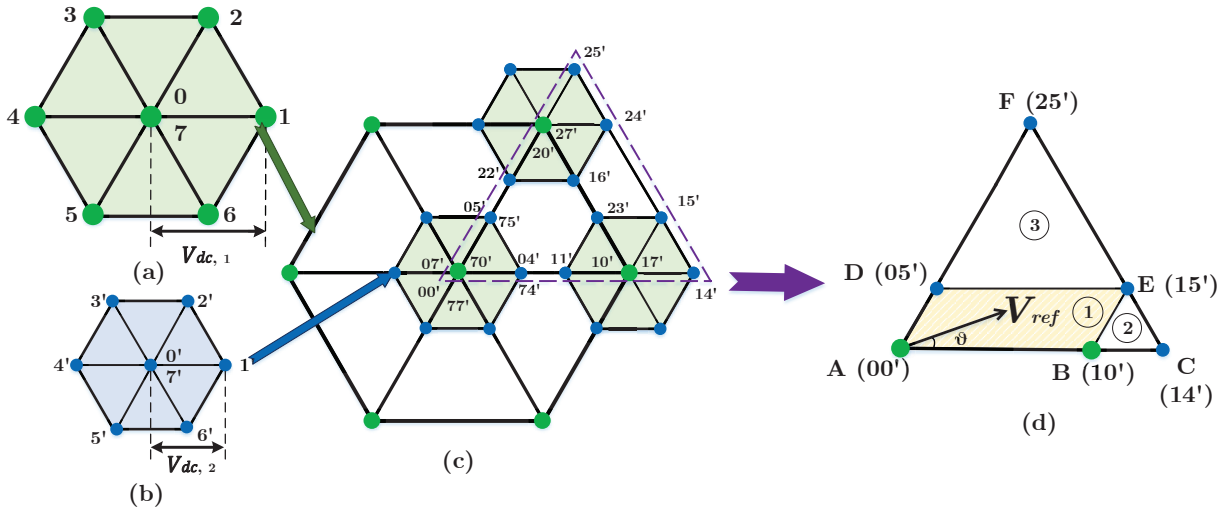


Fig. 2. Space vector diagram for: (a) only CON 1, (b) only CON 2, (c) dual converter (CON 1 + CON 2) and (d) detail of sector I of the unified modulation.

is varying [9].

Therefore, a flexible method known as unified modulation is described in [10] and it is suitable for dual converters with two isolated voltage sources using any positive voltage ratio between the two supplies. In addition, the switching actions of the unified modulation are limited to 2 per switching period, which is lower compared to the 6 actions performed when the two converters are switched simultaneously. This means that the unified modulation technique can considerately reduce the switching loss. Regarding the unified modulation, switching states are separately assigned to each converter, but the studies in [10] have not considered the resulting switching states of the whole dual converter. The states define the modulation shape, which affects the harmonic distortion in the load [11], [12].

This paper presents an enhanced modulation method based on the unified modulation. After a systematic consideration on the switching states of dual converters, the sequences of states assigned to both converters are modified such that the harmonic distortion could be significantly reduced. The effectiveness of the suggested technique has been proved through simulations on an open-end winding induction motor drive.

## II. Operation Principle

Fig.2 illustrates the operation principle employed for obtaining the space vector diagram of dual converter. Each dot represents one switching vector in Fig.2 (a) or (b) and it can be expressed by several switching states, which are known as redundant states. For a two-level converter, as depicted in Fig.2 (a) and (b), the 8 switching states (0-7 or 0'-7') form 7 different vectors in the plane. Since the dual converter employs

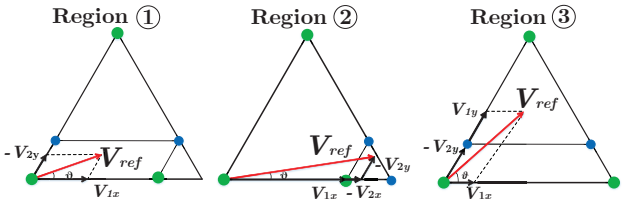


Fig. 3. Vectors synthesis procedure for the dual converter.

two 2-level inverters, there are $8^2 = 64$ applicable switching states.

For the dual converter, the phase voltage applied to the electrical loads is the voltage difference produced by the two converters (CON 1 in Fig.2 (a) and CON2 in Fig.2 (b)). Thus, the voltages applied to the load is obtained by combining the switching states of both converters. For instance, the dual converter switching state (15') is achieved by simultaneously applying the switching states 1 (i.e. switching combination 100) and 5' (i.e. switching combination 001) for CON 1 and CON 2 respectively.

## III. Unified Modulation and Modified Version

### A. Reference vector synthesis

The unified modulation technique synthesizes the reference vector $V_{ref}$ from $V_x$ by CON1 and $V_y$ by CON2, as indicated in Fig.2 (d) [10]. Their corresponding time durations $t_x$ and $t_y$ can be expressed in (1), where $T_s$ is the switching period and $\theta$ is the angle of reference vector $V_{ref}$. Regardless of the voltage ratio of the two converters, the sector, where $V_{ref}$ is located, can always be divided into three regions for modulation proposes, as observable from Fig.2 (d). A more detailed representation of these three regions is provided in

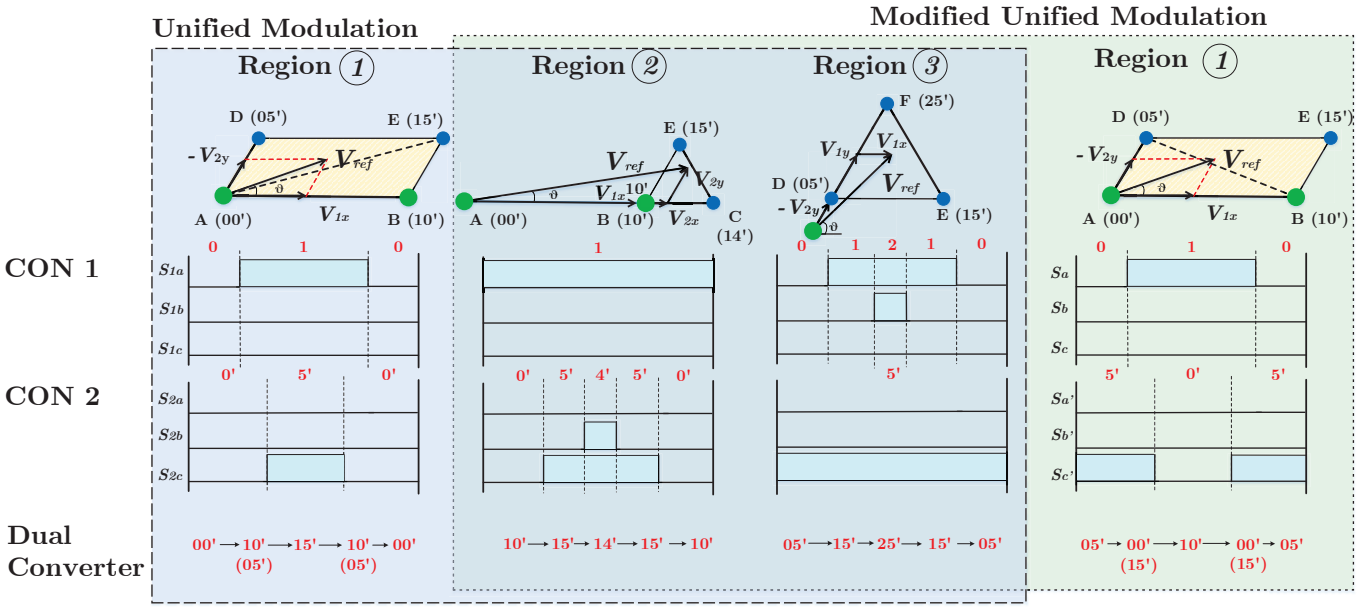


Fig. 4. Switching designs of both unified and proposed modulations.

Fig.3, where the vector synthesis procedure is illustrated. The position of the $V_{ref}$ with respect to the mentioned regions can be identified by comparing $t_x$ and $t_y$ against $T_s$. In case $t_x > T_s$, the $V_{ref}$ lays in region ②, whilst it is situated in region ③ when $t_y > T_s$. Finally, if $t_x < T_s$ and $t_y < T_s$, $V_{ref}$ is found within region ①.

$$t_x = \frac{\sqrt{3} * V_{ref}}{V_{dc,1}} T_s \sin(\pi/3 - \theta) = t_{1x} + t_{2x}$$
$$t_y = \frac{\sqrt{3} * V_{ref}}{V_{dc,2}} T_s \sin\theta = t_{1y} + t_{2y} \quad (1)$$

In (1), the time durations $t_{1x}$, $t_{1y}$ and $t_{2x}$, $t_{2y}$ are assigned to CON1 and CON2, respectively, which correspond to $V_{1x}$, $V_{1y}$ and $V_{2x}$, $V_{2y}$ in Fig.3. If the reference vector $V_{ref}$ locates within region ①, CON1 and CON2 are switching such that $V_{ref}$ is synthesised by $V_{1x}$ and $V_{1y}$, respectively, as indicated in Fig.3. The relevant time duration is expressed in (2). Once the reference vector $V_{ref}$ enters region ②, CON1 is clamped since the time $t_{1x}$ reaches its limit (i.e. $t_{1x} = T_s$), while CON2 will be switched to provide $V_{2x}$ and $V_{2y}$ for $t_{2x}$ and $t_{2y}$, respectively. Under these conditions, the time durations can be derived by (3). As a contrast, when the reference vector $V_{ref}$ moves to region ②, CON2 is now clamped because $t_{2y} = T_s$, whereas CON1 will be switched to form $V_{1x}$ and $V_{1y}$ for $t_{1x}$ and $t_{1y}$, respectively. The corresponding time durations are given by (4).

$$t_{1x} = t_x, t_{2y} = t_y \quad (2)$$

$$t_{2x} = (V_x t_x - V_{1x} T_s)/V_{2x}, t_{2y} = t_y \quad (3)$$

$$t_{1y} = (V_y t_y - V_{2y} T_s)/V_{1y}, t_{1x} = t_x \quad (4)$$

### B. Switching pattern design

Fig.4 presents the switching designs of the unified modulation and the proposed modified version, where $S_{1a}$, $S_{1b}$, $S_{1c}$ and $S_{2a}$, $S_{2b}$, $S_{2c}$ are the switches reported in Fig.1. In addition, the red numbers in Fig.4 refer to the switching states applied by CON1, CON2 and dual converter (i.e. resulting switching state). As displayed in Fig.4, the proposed approach has only changed the modulation within region ①, whereas it has remained the same as for the unified modulation within the other two regions (i.e. ② and ③). In particular, region ① has a parallelogram shape, as denoted ABDE in Fig.4, which needs to be divided into two small triangles for modulation. Indeed, it is commonly recognized that the adoption of regular triangle for modulation would result in superior voltage quality [11].

According to Fig.4, when $V_{ref}$ lays within the region ①, the unified modulation adopts the following switching sequences: A) 0 - 1 - 0 for CON 1, and B) 0' - 5' - 0' for CON 2. Therefore, the switching states of the dual converter could be 00'- 10' - 15' or 00'- 05' - 15'. The first switching sequence (i.e. 00'- 10' - 15') is applied when $t_x > t_y$, while the second one (i.e. 00'- 05' - 15') is employed in case $t_x < t_y$.

However, the problem is the states 00' and 15' will be applied provided that $V_{ref}$ locates within region ①. Consequently, the parallelogram shape of region ① is divided

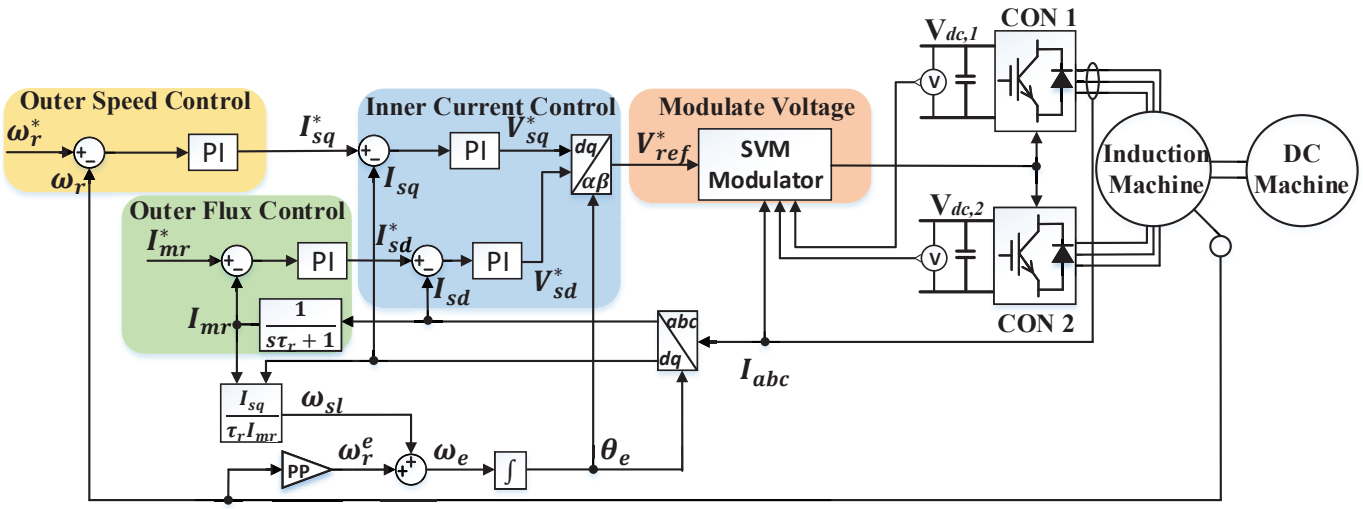


Fig. 5. Control scheme of the motor drive system.

into two obtuse triangles, as shown in ΔABE and ΔADE in Fig.4. Based on the analytical studies regarding the harmonic distortion in [13], the distortion is proportional to the error voltage defined as the difference between applied voltage and the reference vector. Assuming $V_{ref}$ locates near the origin point of space vector diagram, the error voltage between $V_{ref}$ and the vector of state 15' is significantly large. Thus, a significant distortion in the converter output voltage is expected.

Therefore, an approach to appropriately split region ① is necessary for minimizing the voltage harmonic content. In the modified version of unified modulation, the parallelogram of region ① is divided into two acute triangles, which are ΔABD and ΔBDE. As illustrated in Fig.4, the sequence of states 5' and 0' (CON 2) of the unified modulation is swapped, such that 5' is the starting state for the proposed method. Due to the above change, the switching states of the dual converter implementing the introduced modulation strategy become 05' - 00' - 10' or 05' - 15' - 10'. The first switching state (i.e. 05' - 00' - 10') is chosen when $t_x$+$t_y$ <$T_s$, otherwise the second one (i.e. 05' - 15' - 10') is preferred.

## IV. Simulation Results

A simulation model of the motor drive system with dual converter is built within PLECS environment. The detailed parameters of induction machine and power converter are listed in Table I. Fig.5 depicts the closed-loop control scheme of an open-end drive system [14]. This system consists of the main converter (CON 1), the sub converter (CON 2), and an open-end winding induction machine mechanically connected to a DC machine. The classic field orientation control is implemented, where the 'Nested loop' of outer speed and flux controls with inner current control loops is adopted [15].

TABLE I
Machine and Converter Parameters

| Power Converter | | Induction Motor | |
|---|---|---|---|
| CON 1 voltage | 270 V | Stator resistance | 1.2 Ω |
| CON 2 voltage | 270 V | Rotor resistance | 1.01 Ω |
| Switching frequency | 5 kHz | Magnetizing inductance | 0.69 mH |
| Deadtime | 4.1 $\mu$s | Pole number | 2 |

Initially, the voltage and current performance of the dual converter with symmetrical voltage supplies are demonstrated in Fig.6. Two different speed references are considered, which result in as many modulation indexes (M.I.), as defined in (5). From Fig.6, it is clear that the phase voltage obtained by using the unified modulation features undesired voltage steps, which leads to the distorted current performance. In particular, the undesired step is apparent at medium modulation index value, as indicated in Fig.6 (a). In this case, the corresponding phase current would worsen severely. The reason is revealed in Fig.4, where the states 00' and 15' would be both applied in region ①, although the reference vector is far away from either state. By using the proposed method, the states 00' and 15' are automatically selected such that only the one near to the reference vector would be applied for the switching sequence. As proven by the results reported in Fig.6 (b) and (d), the undesired voltage steps are removed when the proposed modulation is implemented. It is apparent that addressed method improves the converter output quality considerately, compared to using the proposed method in [10].

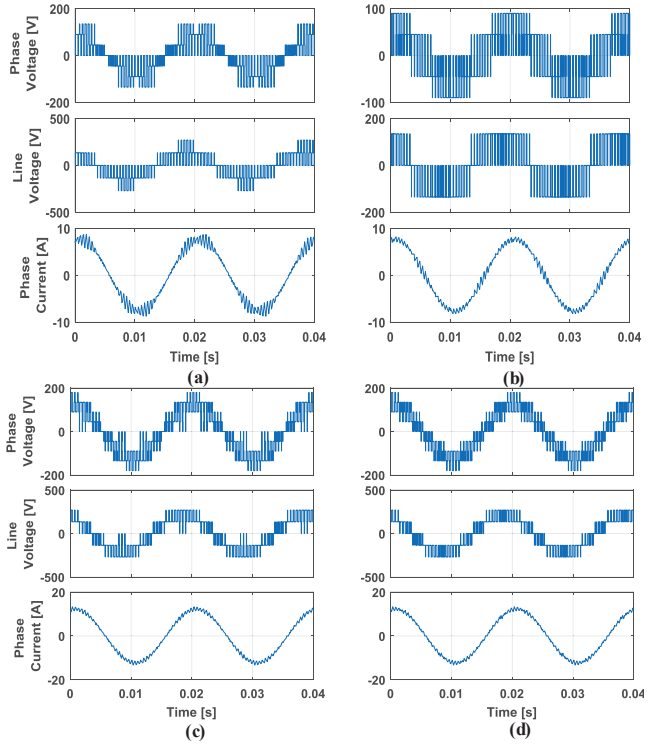


Fig. 6. Voltage and current performance at a) M.I. = 0.5 by unified modulation; b) M.I. = 0.5 by proposed modulation; c) M.I. = 0.8 by unified modulation; b) M.I. = 0.8 by proposed modulation.

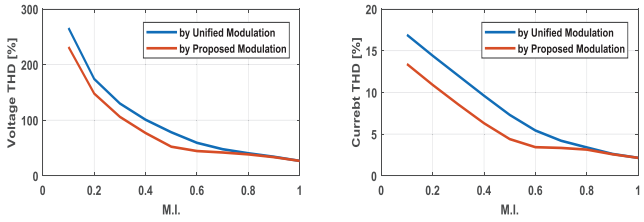


Fig. 7. Voltage and current THD comparison for both unified and proposed modulations.

$$M.I. = \frac{\sqrt{3} * V_{ref}}{V_{dc,1} + V_{dc,2}} \tag{5}$$

In Fig.7, the phase voltage and phase current total harmonic distortion (THD) values are compared for both unified and proposed modulations, in order to verify and quantify the converter output quality improvement achieved through the introduced modulation strategy.

Since the unified modulation could be applied at any positive ratio, the performance comparison for several voltage supplies ratios is also investigated. For instance, the ratios of 2:1 and 3:1 (i.e. asymmetrical voltage supplies) are considered and the phase current waveforms obtained implementing both unified and proposed modulations are compared in Fig.8. These results refer to $M.I. = 0.5$ and confirm that the

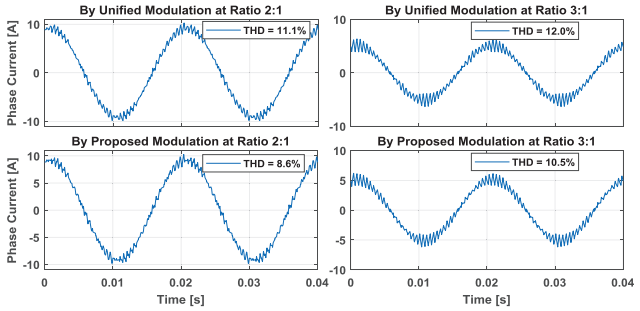


Fig. 8. Current performance of both unified and proposed modulations at M.I.=0.5, in case of asymmetrical voltage supplies.

proposed modulation could still produce output current with lower THD than the unified modulation technique. Hence, the effectiveness of the proposed modulation technique is also demonstrated under asymmetrical voltage supplies conditions.

## V. Conclusion

This paper proposed and discussed an enhanced modulation technique for dual converters with isolated power supplies. Compared to the unified modulation strategy, the proposed technique features an improved output power quality, in terms of both voltage and current waveforms. The benefits rising for the adoption of the presented modulation strategy are significant at small and medium $M.I.$ values. The feasibility of the presented modulation strategy was investigated through an extensive simulation campaign and its and the effectiveness was demonstrated during both symmetrical (i.e. 1:1) and asymmetrical (i.e. 2:1 and 3:1) voltage ratios.

## References


[1] Z. Huang, T. Yang, P. Giangrande, S. Chowdhury, M. Galea, and P. Wheeler, "An active modulation scheme to boost voltage utilization of the dual converter with a floating bridge," *IEEE Transactions on Industrial Electronics*, vol. 66, no. 7, pp. 5623–5633, 2019.

[2] J. R. Aros, R. P. Guíñez, and R. B. Gimenez, "Dual-inverter circuit topologies for supplying open-ended loads," in *Recent Developments on Power Inverters*. InTech, 2017.

[3] W. Zhao, B. Wu, Q. Chen, and J. Zhu, "Fault-tolerant direct thrust force control for a dual inverter fed open-end winding linear vernier permanent-magnet motor using improved svpwm," *IEEE Transactions on Industrial Electronics*, vol. 65, no. 9, pp. 7458–7467, 2018.

[4] M. H. V. Reddy, T. B. Reddy, B. R. Reddy, and M. S. Kalavathi, "Discontinuous pwm technique for the asymmetrical dual inverter configuration to eliminate the overcharging of dc-link capacitor," *IEEE Transactions on Industrial Electronics*, vol. 65, no. 1, pp. 156–166, 2018.

[5] S. Chowdhury, P. Wheeler, Z. Huang, M. Rivera, and C. Gerada, "Fixed switching frequency predictive control of an asymmetric source dual inverter system with a floating bridge for multilevel operation," *IET Power Electronics*, vol. 12, no. 3, pp. 450–457, 2019.

[6] Y.-f. Jia, N. Xu, L. Chu, L.-f. Zhang, D. Zhao, Y.-k. Li, and Z.-h. Yang, "Power flow control strategy based on the voltage vector distribution for a dual power electric vehicle with an open-end winding motor drive system," *IEEE Access*, 2018.

[7] S. Jayasinghe and D. Vilathgamuwa, "Dual inverter system with integrated energy storage for grid connected photovoltaic systems," in *Power Electronics and Drive Systems (PEDS), 2015 IEEE 11th International Conference on*, pp. 796–803. IEEE, 2015.

[8] M. Chen and D. Sun, "A coordinated svpwm without sector identification for dual inverter fed open winding ipmsm system," in *Energy Conversion Congress and Exposition (ECCE), 2016 IEEE*, pp. 1–8. IEEE, 2016.

[9] C. I. Hill, S. Bozhko, T. Yang, P. Giangrande, and C. Gerada, "More electric aircraft electro-mechanical actuator regenerated power management," in *2015 IEEE 24th International Symposium on Industrial Electronics (ISIE)*, pp. 337–342, Jun. 2015.

[10] M. Chen and D. Sun, "A unified space vector pulse width modulation for dual two-level inverter system," *IEEE Transactions on Power Electronics*, vol. 32, no. 2, pp. 889–893, 2017.

[11] B. P. McGrath, D. G. Holmes, and T. Lipo, "Optimized space vector switching sequences for multilevel inverters," *IEEE Transactions on power electronics*, vol. 18, no. 6, pp. 1293–1301, 2003.

[12] Z. Huang, T. Yang, P. Giangrande, P. Wheeler, and M. Galea, "An effective hybrid space vector pwm technique to improved inverter performance," in *2017 IEEE Southern Power Electronics Conference (SPEC)*, pp. 1–6. IEEE, 2017.

[13] G. Narayanan, D. Zhao, H. K. Krishnamurthy, R. Ayyanar, and V. Ranganathan, "Space vector based hybrid pwm techniques for reduced current ripple," *IEEE Transactions on Industrial Electronics*, vol. 55, no. 4, pp. 1614–1627, 2008.

[14] P. Giangrande, C. Hill, S. Bozhko, and C. Gerada, "A novel multi-level electro-mechanical actuator virtual testing and analysis tool," in *7th IET Conference on Power Electronics, Machines and Drives*, pp. 1–6. IET, 2014.

[15] P. Giangrande, A. Galassini, S. Papadopoulos, A. Al-Timimy, G. Lo Calzo, M. Degano, and M. Gerada, Christopher Galea, "Considerations on the development of an electric drive for a secondary flight control electromechanical actuator," *IEEE Transactions on Industry Applications*, http://dx.doi.org/10.1109/TIA.2019.2907231DOI 10.1109/TIA.2019.2907231, pp. 1–1, 2019.